Published in final edited form as:
Cell Host Microbe. 2009 November 19; 6(5): 422–432. doi:10.1016/j.chom.2009.09.012.

Two mechanistically distinct immune evasion proteins of cowpox virus combine to avoid antiviral CD8 T cells

Minji Byun[1], **Marieke C. Verweij**[3], **David J. Pickup**[5], **Emmanuel J. H. J. Wiertz**[3,4], **Ted H. Hansen**[2], and **Wayne M. Yokoyama**[1,2,6]

[1] Division of Rheumatology, Department of Medicine, Washington University School of Medicine, St. Louis, MO 63110, USA [2] Department of Pathology and Immunology, Washington University School of Medicine, St. Louis, MO 63110, USA [3] Department of Medical Microbiology and Center of Infectious Diseases, Leiden University Medical Center, Leiden, The Netherlands [4] Department of Medical Microbiology, University Medical Center Utrecht, Utrecht, The Netherlands [5] Department of Molecular Genetics and Microbiology, and Duke Human Vaccine Institute, Duke University Medical Center, Durham, NC 27710, USA [6] Howard Hughes Medical Institute

Summary

Downregulation of MHC class I on the cell surface is an immune evasion mechanism shared by many DNA viruses including cowpox virus. Previously, a cowpox virus protein, CPXV203, was shown to downregulate MHC class I. Here, we report that CPXV12 is the only other MHC class I regulating protein of cowpox virus and it uses a mechanism distinct from that of CPXV203. Whereas CPXV203 retains fully assembled MHC class I by exploiting the KDEL-mediated endoplasmic reticulum retention pathway, CPXV12 binds to the peptide-loading complex and inhibits peptide loading on MHC class I molecules. Viruses deleted of both CPXV12 and CPXV203 demonstrated attenuated virulence in a CD8 T cell-dependent manner. These data demonstrate that CPXV12 and CPXV203 proteins combine to ablate MHC class I expression and abrogate antiviral CD8 T cell responses.

Introduction

Major histocompatibility complex (MHC) class I molecules play a critical role in antiviral immunity. A MHC class I molecule is composed of a heavy chain, a β2-microglobulin (β2m) light chain, and a peptide of 8 to 10 amino acids in length. The majority of MHC class I-binding peptides is generated in the cytosol by proteasomes and transported into the lumen of the endoplasmic reticulum (ER) by transporter associated with antigen processing (TAP). Peptide loading onto the MHC class I heavy chain-β2m heterodimer is facilitated by a multisubunit protein complex called the MHC class I peptide-loading complex (PLC) (Peaper and Cresswell, 2008). In addition to TAP and MHC class I, the PLC is composed of ER chaperones such as tapasin, ERp57, calreticulin, and protein disulfide isomerase. Upon peptide loading, the fully assembled MHC class I complexes dissociate from the PLC and transit to the cell surface. Recognition of viral peptides in the context of MHC class I molecules triggers virus-specific CD8 T cells to exert their effector functions including cytotoxicity and cytokine secretion (Guidotti and Chisari, 1996).

Contact: Tel: 1-314-362-9075, Fax 1-314-362-9257, yokoyama@im.wustl.edu.

To avoid detection by CD8 T cells, viruses have evolved various mechanisms to interfere with MHC class I antigen presentation (Hansen and Bouvier, 2009). Some viruses accelerate MHC class I turnover. Human cytomegalovirus (HCMV) US2 and US11 cause proteasomal degradation of MHC class I molecules by retrograde transport from the ER to the cytosol (Wiertz et al., 1996a; Wiertz et al., 1996b). The mK3 protein of murine gamma-herpesvirus 68 (MHV-68) induces proteasomal degradation of MHC class I as well as other components of the PLC (Boname et al., 2004; Lybarger et al., 2003; Stevenson et al., 2000). Kaposi's sarcoma-associated herpesvirus (KSHV) K3 and K5, murine cytomegalovirus (MCMV) m06/gp48, and myxoma virus leukemia-associated protein induce lysosomal degradation of MHC class I (Coscoy and Ganem, 2000; Guerin et al., 2002; Ishido et al., 2000; Reusch et al., 1999; Zuniga et al., 1999). An alternative strategy is retention of MHC class I molecules in the ER or ER-Golgi intermediate compartments. Adenovirus E3/19K, HCMV US3, and MCMV m152/gp40 fall into this category (Ahn et al., 1996a; Andersson et al., 1985; Jones et al., 1996; Liu et al., 2007; Ziegler et al., 1997). TAP appears to be an attractive target for viral inhibition of MHC class I biosynthesis. Herpes simplex virus (HSV) ICP-47 (Fruh et al., 1995; Hill et al., 1995; York et al., 1994), HCMV US6 (Ahn et al., 1997; Hengel et al., 1997; Lehner et al., 1997), varicellovirus UL49.5 (Koppers-Lalic et al., 2005; Koppers-Lalic et al., 2008), and BNLF2a of Epstein-Barr virus (Hislop et al., 2007) were shown to interfere with TAP function to limit the supply of peptides for loading onto MHC class I. These viral inhibitors of MHC class I expression have yielded insight into normal MHC class I synthesis and assembly.

The *in vivo* significance of these viral MHC class I evasion mechanisms however, is not well understood and somewhat controversial. In a mouse model of HSV-1, ICP-47 was shown to enhance neurovirulence (Goldsmith et al., 1998). However, this data should to be interpreted with caution because ICP-47 has minimal effect on murine MHC class I (Ahn et al., 1996b). MHV-68 and MCMV, on the other hand, efficiently inhibit murine MHC class I. Whereas mK3-deficient MHV-68 failed to establish a normal latent load (Stevenson et al., 2002), MCMV lacking all known MHC class I evasion genes (m04, m06, m152) did not demonstrate attenuated virulence unless they were tested in immunocompromised or newborn mice (Doom and Hill, 2008). Furthermore, to our knowledge, it has not been clearly demonstrated how the evasion of MHC class I antigen presentation affects the pathogenesis of non-herpesviruses.

In this regard, it is noteworthy that cowpox virus (CPXV) has recently been shown to downregulate MHC class I and evade antiviral CD8 T cell responses (Dasgupta et al., 2007). CPXV belongs to *Orthopoxvirus* genus of the poxvirus family, which also includes other clinically important pathogens such as variola virus, the causative agent of smallpox, and monkeypox virus. Wild rodents are believed to be the natural reservoir hosts of CPXV in Europe (Chantrey et al., 1999). Like other orthopoxviruses, CPXV encodes a large number of immune evasion genes in its DNA genome (Seet et al., 2003). One of such genes, CPXV203, was shown to have a role in MHC class I downregulation by CPXV (Byun et al., 2007). It was identified by screening murine cell lines expressing selected candidate genes for gain-of-function, i.e., MHC class I downregulation. We demonstrated that CPXV203 interferes with the intracellular trafficking of MHC class I molecules by sequestering them in the ER using its C-terminal KDEL-like sequence. However, CPXV203-deficient virus (CPXVΔ203) still efficiently downregulated MHC class I molecules on the cell surface, indicating the virus encodes another, yet to be identified, MHC class I modulator(s).

Here, we report that CPXV12 is responsible for the residual MHC class I downregulation by CPXVΔ203. Based on biochemical studies, we demonstrate that CPXV12 inhibits MHC class I expression by impairing ER peptide loading and dissociation of MHC class I from TAP. Importantly, using a mouse model, we provide evidence that MHC class I downregulation by

CPXV12 and CPXV203 contributes to CPXV virulence by ablating antiviral CD8 T cell responses.

Results

Identification of CPXV12 by loss-of-function screening

To find another CPXV gene(s) with MHC class I downregulating activity, we undertook a strategy different from that used to identify CPXV203. In a loss-of-function screening approach, we examined A518, a CPXV mutant in which 28.5 kb region between the ClaI sites at positions 10642 and 39152 had been deleted (Fig. 1A). Since A518 contains intact CPXV203, we generated its derivative deleted of CPXV203 (A518Δ203) to investigate CPXV203-independent MHC class I downregulating activity (Fig. 1A). Murine fibroblast MC57G cells were infected with A518Δ203, and their surface MHC class I levels were compared to those of CPXVΔ203-infected cells. GFP inserted in the CPXV203 locus enabled detection of the virus-infected cells by flow cytometry. Downregulation of K^b and D^b was observed in CPXVΔ203-infected cells, as we previously reported, but not in A518Δ203-infected cells (Fig. 1B). These data indicated the genomic region deleted in A518 contains the gene(s) responsible for the residual MHC class I downregulating activity of CPXVΔ203.

The genomic region deleted in A518 contains 26 open reading frames (ORFs) from CPXV11 to CPXV36. To map the MHC class I downregulating activity among these ORFs, we split them into two groups, CPXV11-21 and CPXV22-36, and generated recombinant viruses specifically lacking each group of genes in addition to CPXV203. When these viruses were tested for the ability to downregulate K^b, CPXVΔ11-21Δ203, but not CPXVΔ22-36Δ203, recapitulated the loss-of-function phenotype of A518Δ203, narrowing down the candidate region to CPXV11-CPXV21 (Fig. 1C). After four iterative rounds of paired deletion-mutant screening, we found that deletion of the genomic region encoding CPXV12 is sufficient to prevent K^b downregulation by CPXVΔ203 (Fig. 1C and 1D). Similarly, CPXVΔ203-mediated downregulation of D^b and D^k was abrogated by the deletion of CPXV12 (Fig. 1D). Therefore, CPXV12 is responsible for the CPXV203-independent MHC class I downregulating activity of CPXV.

CPXV12 delays the intracellular trafficking of MHC class I

The loss of MHC class I downregulating activity by the deletion of CPXV12 did not exclude the possibility that the protein encoded by CPXV12 might depend on other viral proteins for its function. To investigate this issue, we expressed CPXV12 in the absence of other CPXV proteins in murine lymphoblast C1498 cells using a bicistronic retroviral expression vector containing an internal ribosomal entry site followed by GFP. There was good correlation between the expression of CPXV12, which was inferred from GFP expression, and the reduction of K^b and D^b levels, demonstrating that CPXV12 is sufficient for MHC class I downregulation (Fig. 2A).

The deduced sequence of CPXV12 consists of 69 amino acids, and does not exhibit any similarity with other viral or mammalian proteins except its orthologs in CPXV strain GRI-90, Germany 91-3, and ectromelia virus (ECTV) strain Moscow. Sequence homology between CPXV12 and its poxvirus orthologs is significant only for the N-terminal region, which contains a putative transmembrane domain (Supplemental fig. 1A). Expression of the ECTV ortholog EVM007 in C1498 cells did not induce MHC class I downregulation (Supplemental fig. 1B), suggesting the function of CPXV12 might have diverged from that of its orthologs during evolution.

To understand the mechanism by which CPXV12 modulates MHC class I expression, we monitored the biosynthesis of MHC class I by pulse-chase experiments. Similar amounts of K^b heavy chains were synthesized in vector- and CPXV12-transduced cells during the labeling period, indicating the *de novo* synthesis of MHC class I was unaffected by CPXV12 (Fig. 2B, chase 0 min). However, we found markedly slower accumulation of Endo H-resistant K^b (Fig. 2B) and D^b (data not shown) in CPXV12-transduced cells. Since glycoproteins acquire Endo H-resistance during transit through the Golgi, these data indicated CPXV12 inhibits the intracellular trafficking of newly synthesized MHC class I molecules.

Consistent with these data, the steady-state level of Endo H-resistant K^b heavy chain was markedly lower in CPXV12-expressing cells (CPXV12-transduced C1498 cells or CPXVΔ203-infected MC57G cells), compared to their respective control cells (vector-transduced C1498 cells or CPXVΔ12Δ203-infected MC57G cells) (Fig. 2C). Together, these results suggested that the reduction of MHC class I levels on the cell surface is likely due to a defect in intracellular trafficking induced by CPXV12.

CPXV12 inhibits the release of MHC class I from the PLC

We hypothesized that the delayed trafficking of MHC class I molecules in CPXV12-expressing cells might be due to PLC dysfunction, since the PLC is responsible for the quality-control of MHC class I assembly, ensuring only optimally assembled MHC class I molecules are released from the ER. To test this hypothesis, we first examined whether CPXV12 physically interacts with the PLC by co-immunoprecipitation experiments. CPXV12 tagged with a hemagglutin (HA)-epitope at the C-terminus (CPXV12-HA) was expressed in C1498 cells. Precipitation of CPXV12-HA with anti-HA antibody co-precipitated TAP1, tapasin, and K^b heavy chain (Fig. 3A). Reciprocally, immunoprecipitation with anti-TAP1 serum co-precipitated CPXV12-HA along with other components of the PLC (Fig. 3A). Together, these results suggested that CPXV12 physically associates with the PLC without disrupting its overall assembly.

Examination of the anti-TAP1 precipitates also revealed that the levels of TAP1, tapasin, and calreticulin in the PLC were unaffected, whereas the level of PLC-associated K^b heavy chain was dramatically increased in CPXV12-transduced cells (Fig. 3A). These results were further validated by performing similar experiments with CPXV-infected cells. The level of PLC-associated K^b heavy chain was strikingly higher in CPXVΔ203-infected cells (CPXV12-sufficient) compared to CPXVΔ12Δ203-infected cells (CPXV12-deficient) (Fig. 3A).

To investigate this further, we examined the kinetic profile of PLC-MHC class I interaction. In vector-transduced cells, the level of PLC-associated K^b heavy chain peaked at 10 min after the initial synthesis, and then gradually diminished over time (Fig. 3B). This pattern was consistent with the transient interaction between the newly synthesized MHC class I molecules and the PLC during the peptide loading process. In CPXV12-transduced cells, the level of PLC-associated K^b also peaked at 10 min, but it was sustained for at least 50 min without decrease (Fig. 3B). These data demonstrated that CPXV12 inhibits the dissociation of MHC class I molecules from the PLC.

CPXV12 impairs peptide loading

The prolonged interaction between MHC class I and the PLC in CPXV12-transduced cells suggested a defect in the peptide loading process. To test this, we evaluated the thermostability of peptide-MHC class I complex, which has been shown to reflect peptide affinity (Bouvier and Wiley, 1994; Fahnestock et al., 1992; Schumacher et al., 1990; Williams et al., 2002). Most K^b molecules in vector-transduced cells withstood 37°C incubation without losing their intact conformation, whereas K^b molecules in CPXV12-transduced cells failed to maintain their conformation unless they were pre-incubated with high-affinity peptide VNVDYSKL (Fig.

4A). These results suggested that MHC class I molecules in CPXV12-transduced cells were loaded with suboptimal peptides.

Furthermore, we found that MHC class I molecules in CPXV12-transduced cells were peptide-receptive. Exogenously added SIINFEKL peptides that bind to K^b with high affinity restored the surface expression of K^b in CPXV12-transduced cells in a dose-dependent manner (Fig. 4B). This was due to a specific interaction between MHC class I and its cognate peptide because the incubation with D^b-binding peptide ASNENMETM had no effect on K^b expression (Fig. 4B), whereas it restored D^b expression (data not shown). Together, these data suggested that CPXV12 inhibits optimal peptide loading on MHC class I.

Impaired peptide loading could be a result of insufficient peptide supply in the ER. The majority of MHC class I binding peptides are transported from the cytosol into the ER by TAP, and we found a statistically significant reduction of TAP-dependent peptide transport activity in CPXV12-transduced C1498 cells (Fig. 4C). However, the reduction was rather modest, especially compared to the effect of UL49.5 (Fig. 4C), a potent inhibitor of TAP encoded by bovine herpesvirus 1 (BHV-1) (Koppers-Lalic et al., 2005). Yet, we observed a similar degree of MHC class I downregulation in UL49.5- and CPXV12-expressing cells (Fig. 4D), suggesting CPXV12 has additional mechanisms of impairing peptide loading independent of regulating peptide supply.

Notably, CPXV203 did not compromise the thermostability of K^b (Fig. 4A), which was in line with the previous observation that exogenously added peptides did not reverse MHC class I downregulation by CPXV203 (Byun et al., 2007). Together, these results indicate that CPXV12 and CPXV203 use different mechanisms to block MHC class I expression. CPXV12 engages MHC class I prior to full assembly and impairs peptide binding and TAP dissociation, whereas CPXV203 engages MHC class I after TAP dissociation and exploits an ER retrieval pathway.

Evasion of CD8 T cells by CPXV12 and CPXV203

The discovery that CPXV encodes two proteins that downregulate MHC class I with distinct mechanisms prompted us to investigate the relative contribution of each of these proteins in MHC class I regulation and *in vivo* infection. MC57G cells infected with wild-type CPXV (wtCPXV) or viruses deleted of either or both CPXV12 and CPXV203 (CPXVΔ12, CPXVΔ203, CPXVΔ12Δ203) were compared for their MHC class I levels on the cell surface. To ensure the multiplicity of infection was comparable between the viruses, poxvirus HA levels were measured as controls. Deletion of either CPXV12 or CPXV203 alone did not have a notable effect except the partial increase of K^b expression by the deletion of CPXV203 compared to wtCPXV (Fig. 5A). However, deletion of both proteins completely abrogated the downregulation of K^b and D^b by CPXV, confirming that they are the only components of CPXV involved in MHC class I downregulation.

Since a primary role of MHC class I molecules is presenting antigens to CD8 T cells, we examined the effect of CPXV12 and CPXV203 on the antiviral CD8 T cell response. Splenocytes from wtCPXV-infected C57BL/6 mice were harvested at day 7 post infection and stimulated with MC57G cells that were infected with wtCPXV or CPXV deletion-mutants *in vitro*. We found good correlation between the MHC class I levels on the target cells and the size of CD8 T cell responses. MC57G cells infected with wtCPXV or CPXVΔ12, which displayed very low levels of K^b and D^b (Fig. 5A), were extremely poor at stimulating CD8 T cells for IFN-γ production (Fig. 5B and 5C) or cytotoxicity (Fig. 5D). In comparison, CPXVΔ203-infected MC57G cells, which expressed higher levels of K^b than wtCPXV- or CPXVΔ12-infected cells (Fig. 5A), triggered a larger number of CD8 T cells to produce IFN-γ and exert cytotoxicity (Fig. 5B–5D). Importantly, CPXVΔ12Δ203-infected cells, which expressed much higher levels of K^b and D^b than any other virus-infected group, were most

efficient at stimulating IFN-γ and cytotoxicity of CD8 T cells (Fig. 5B–5D). Together, these results demonstrated that CPXV12 and CPXV203 protect CPXV-infected cells from antiviral CD8 T cell responses, likely by downmodulating MHC class I.

CPXV12 and CPXV203 contribute to virulence by evading CD8 T cells *in vivo*

To investigate the *in vivo* roles of CPXV12 and CPXV203, naïve 9-week-old C57BL/6 mice were infected with 5×10^4 PFU of wtCPXV, CPXVΔ12Δ203, or revertant virus ($CPXV^R12^R203$) via an intranasal route and monitored for survival. All mice infected with either wtCPXV or $CPXV^R12^R203$ succumbed to disease between 9–14 days post infection, while 19 of 20 (95%) CPXVΔ12Δ203-infected mice survived (Fig. 6A). These data clearly demonstrated the important contributions of CPXV12 and CPXV203 in CPXV virulence in the host.

The attenuation of CPXVΔ12Δ203 could be due to a loss of intrinsic replication potential. However, in Vero cells cultured *in vitro*, CPXVΔ12Δ203 replicated with similar kinetics compared to wtCPXV and $CPXV^R12^R203$ as measured by one-step growth curve (Fig. 6B), indicating CPXV12 and CPXV203 are not essential for intracellular virus replication. Furthermore, we did not find a significant difference in spleen titers between wtCPXV- or CPXVΔ12Δ203-infected groups at day 7 post infection (Fig. 6C), which also argued against an intrinsic defect in replication as the reason for the decreased virulence of CPXVΔ12Δ203. Rather, the significantly lower viral titers in CPXVΔ12Δ203-infected animals at day 10 post infection suggested that the host immune system could clear the viruses more efficiently in the absence of CPXV12 and CPXV203 (Fig. 6C).

Based on these *in vivo* data as well as the *in vitro* data examining the influence of CPXV12 and CPXV203 on the antiviral functions of CD8 T cells, we hypothesized that the attenuation of CPXVΔ12Δ203 might be due to its inability to evade CD8 T cells. To test this hypothesis, we compared the virulence of wtCPXV and CPXVΔ12Δ203 in CD8-depleted mice. C57BL/6 mice treated with either isotype-control or CD8-depleting antibody were infected with 1×10^4 PFU of wtCPXV or CPXVΔ12Δ203. In control-depleted mice, CPXVΔ12Δ203 was less virulent than wtCPXV (Fig. 6D), consistent with the data obtained with higher dose of virus inoculum (Fig. 6A). By contrast, in CD8-depleted mice, CPXVΔ12Δ203 was no longer attenuated compared to wtCPXV (Fig. 6D). Furthermore, the comparison of mortality rates between control- or CD8-depleted groups demonstrated that CD8 T cells had little protective effect against CPXV in the presence of CPXV12 and CPXV203, whereas they were protective in the absence of CPXV12 and CPXV203 (Fig. 6D). Together, these data provide compelling evidence that CPXV12 and CPXV203 contribute to CPXV virulence by inhibiting the antiviral CD8 T cell responses.

Discussion

CPXV203 was the first CPXV protein shown to be involved in MHC class I downregulation, but the deletion of CPXV203 did not fully abolish the phenotype, indicating CPXV encodes another protein with similar function. Here, we mapped the CPXV203-independent MHC class I downregulating activity of CPXV to CPXV12 by loss-of-function screening of deletion-mutant viruses. Furthermore, we showed that expression of CPXV12 alone, independent of other CPXV genes, is sufficient for MHC class I downregulation. Together, these results provide genetic and biochemical evidence that CPXV12 is a bona fide immunomodulatory gene targeting MHC class I molecules.

Our combined data illustrate the mechanism by which CPXV12 inhibits MHC class I expression on the cell surface. CPXV12 does not affect the initial translation of MHC class I molecules, but it delays their maturation. The poor thermostability of MHC class I in CPXV12-

expressing cells suggests that CPXV12 inhibits peptide loading, which also explains the retention of MHC class I molecules by the PLC. A clear co-precipitation of CPXV12 with the PLC strongly suggests CPXV12 interacts with one or more component(s) of the PLC, which has yet to be identified, but the interaction does not disrupt the assembly of the PLC. Since tapasin is required for stable expression of TAP, this finding rules out the possibility that the modest inhibition of peptide transport by TAP results from CPXV12 disrupting tapasin/TAP interaction. Thus we favor the notion that CPXV12 interferes with peptide loading by binding to either tapasin or MHC class I and impairs tapasin-facilitated peptide binding to MHC class I. If this model is correct, further investigation of CPXV12 might shed a light on our understanding of the molecular details of how the PLC orchestrates peptide loading of MHC class I and what induces the dissociation of fully assembled MHC class I from TAP.

Viruses deleted of both CPXV12 and CPXV203 exhibited a complete loss-of-function phenotype, indicating the two proteins are the major effectors of CPXV-mediated MHC class I downregulation. Interestingly, they are structurally and mechanistically divergent. They do not share sequence homology either at the nucleotide or at the amino acid level. They have different topologies; CPXV12 is likely a type II-membrane protein with a short cytoplasmic domain (~10 residues) and a longer luminal domain (~34 residues), whereas CPXV203 is likely a soluble protein with a cleavable N-terminal signal peptide. The mechanisms by which they interfere with MHC class I biosynthesis are also different. CPXV12 impairs peptide loading, while CPXV203 exploits a physiologic ER retention mechanism to retain peptide-loaded MHC class I molecules in the ER. Thus, CPXV12 and CPXV203 must have evolved independently rather than sharing a common ancestor, and yet, they have acquired similar function, implying the importance of MHC class I antigen presentation and antiviral CD8 T cell response in host defense against CPXV.

The effects of CPXV12 and CPXV203 on sequential steps of MHC class I biosynthesis pathway suggest that they may work synergistically. Limiting the number of peptide-loaded MHC class I molecules in the ER by CPXV12 would reduce the burden of CPXV203, allowing tighter control of MHC class I trafficking. Furthermore, the two proteins may have a different allele-specific hierarchies in their effects on MHC class I expression, as it was observed for the various MHC class I inhibitors encoded by HCMV (Machold et al., 1997) or MCMV (Wagner et al., 2002). Such complementation between the two proteins will ensure broad yet potent MHC class I downregulating activity and counterbalance evolution of host MHC class I molecules to avoid effects of any single CPXV protein.

Identification of all major CPXV proteins involved in MHC class I downregulation allowed us to examine the physiological role of this immune evasion mechanism. The superior virulence of wtCPXV compared to CPXVΔ12Δ203 in wild-type mice, but not in CD8 T cell depleted mice, demonstrates that CPXV12 and CPXV203 enhance CPXV virulence by abrogating antiviral CD8 T cell responses. Interestingly, depletion of CD8 T cells had little effect against wtCPXV. This may seem paradoxical since the premise of MHC class I downregulation is to block antiviral CD8 T cell responses. However, by removing CPXV12 and CPXV203, we were able to confirm that CD8 T cells confer protection against CPXV *in vivo*. The critical role of CD8 T cells was also demonstrated for ECTV, an orthopoxvirus closely related to CPXV, which does not encode any known evasion mechanism targeting MHC class I molecules. Like in the CPXVΔ12Δ203-infected animals, depletion of CD8 T cells was detrimental for the survival of ECTV-infected animals (Karupiah et al., 1996). Taken together, these data highlight the remarkable ability of CPXV12 and CPXV203 to neutralize antiviral immunity mediated by CD8 T cells.

Although the molecular mechanisms of MHC class I downregulation encoded by other viruses have been extensively studied, demonstrating the *in vivo* significance has been challenging.

We think our experimental system is ideal to study the *in vivo* role of virus-induced MHC class I downregulation for several reasons. First, mice are biologically relevant hosts for CPXV, since the natural reservoirs of CPXV are wild rodents. Second, C57BL/6 strain of mice used for our studies express MHC class I molecules of H-2^b haplotype, which are very susceptible to CPXV-induced downregulation. Third, CPXV seems to have effective measures to counteract NK cells. While MHC class I downregulation prevents activation of CD8 T cells, it provokes NK cells due to the reduced engagement of NK inhibitory receptors. This could potentially 'neutralize' the *in vivo* phenotype caused by the effect on CD8 T cells. However, in CD8-depleted animals, where MHC class I downregulation would only affect the NK cell response, we did not find difference in virulence between wtCPXV and CPXVΔ12Δ203. Perhaps this is due to other CPXV immunomodulatory proteins, such as orthopoxvirus MHC class I-like protein (OMCP) that acts as a competitive antagonist of an NK cell activating receptor NKG2D (Campbell et al., 2007). Together, these factors allowed us to clearly demonstrate the significant impact of MHC class I downregulation on the disease outcome.

The data presented here also have interesting implications on the relative contribution of direct priming versus cross-priming in generation of antiviral CD8 T cells during CPXV infection. We noted that CPXV-primed CD8 T cells are easily detectable in the spleens of wtCPXV-infected mice. Since MHC class I downregulation is predicted to disable direct priming, this result suggests an active role of cross-priming. In any case, the findings reported here further accentuate the value of the CPXV model system to study host-pathogen interactions.

Experimental Procedures

Cell lines and virus

Cell lines MC57G, C1498, Vero, and CV-1 were obtained from American Type Culture Collection (ATCC), and cultured in ATCC-recommended media. CPXV strain Brighton Red (CPXV-BR) was obtained from ATCC and propagated in Vero cells. Viruses were purified from the infected Vero cell lysates by centrifugation through 36% sucrose solution. Viral titers were quantified by plaque assay using CV-1 cells.

Flow cytometry

The following monoclonal antibodies were used for flow cytometry: 28-14-8 for D^b (Abcam), AF6-88.5 for K^b, KH95 for D^b, XMG1.2 for IFN-γ (all from BD Biosciences), 53-6.7 for CD8α (eBioscience), and IH831 (a gift of G. Karupiah, Australian National University) for poxvirus HA. For intracellular staining of IFN-γ, cells were fixed and permeabilized using Cytofix/Cytoperm solution (BD Biosciences). All flow cytometric data were collected using a FACSCalibur (BD Biosciences) and analyzed with FlowJo software (Tree Star).

Generation of recombinant viruses

A518 is a deletion variant of CPXV-BR in which the 28.5 kb region between the ClaI sites at positions 10,642 and 39,152 have been replaced with the selectable marker gene Escherichia coli guanine phosphoribosyltransferase (*gpt*). The detailed protocol of A518 generation is described in the supplemental data. A518Δ203, a derivative of A518 with deletion of CPXV203, was generated using a method previously described for the generation of CPXVΔ203 (Byun et al., 2007).

To generate the recombinant viruses used for the mapping experiments (CPXVΔ11-21Δ203, CPXVΔ22-36Δ203, CPXVΔ11-17Δ203, CPXVΔ18-21Δ203, CPXVΔ11-15Δ203, CPXVΔ16-17Δ203, CPXVΔ11-12Δ203, CPXVΔ13-15Δ203, CPXVΔ11Δ203, and CPXVΔ12Δ203), 5′ and 3′ flanking sequences (each 500 bp-long) of the genomic regions targeted for deletion were cloned from CPXV genomic DNA into pBluscriptII (Stratagene).

Between the flanking sequences, VVpI1L-GFP, a GFP expression cassette under the vaccinia virus I1L promoter (Liu et al., 2004), was inserted. CPXVΔ203-infected CV-1 cells were transfected with the targeting plasmids, and the recombinant viruses were isolated from GFP-positive plaques. Desired mutations were confirmed by PCR.

TDS method was adapted to generate CPXVΔ12, CPXVΔ12Δ203, and the revertant $CPXV^{R}12^{R}203$. Two selection cassettes, VVpI1L-GFP and the vaccinia virus 7.5K promoter driven *gpt*, were inserted into pBluscriptII generating a selection plasmid we termed pTDS. 5′ and 3′ flanking sequences of CPXV12 were amplified and sewed together by PCR, and inserted into the pTDS. This plasmid, pTDSΔ12, was transfected into CV-1 cells that were infected with wtCPXV or CPXVΔ203 to generate CPXVΔ12 or CPXVΔ12Δ203, respectively. To generate $CPXV^{R}12^{R}203$, CPXV12 and CPXV203 were sequentially reverted from CPXVΔ12Δ203. Targeting plasmids, $pTDS^{R}12$ and $pTDS^{R}203$, were constructed by cloning the genomic segments spanning CPXV12 or CPXV203 (from 500 bp-upstream to 500 bp-downstream of the coding sequence) into pTDS, respectively. First, CPXV12 locus was reverted by transfecting $pTDS^{R}12$ into CPXVΔ12Δ203-infected CV-1 cells, generating $CPXV^{R}12\Delta203$. $CPXV^{R}12\Delta203$-infected CV-1 cells were then transfected with $pTDS^{R}203$ to generate $CPXV^{R}12^{R}203$.

Retroviral transduction

CPXV12 was cloned from CPXV genomic DNA into pMXsIG (T. Kitamura, University of Tokyo), a retroviral expression vector with internal ribosomal entry site followed by GFP, which was then transfected into Plat-E cells (T. Kitamura, University of Tokyo) using FuGENE6 (Roche). The gene encoding BHV-1 UL49.5 was cloned into the pLZRSΔNGFR vector as described (Koppers-Lalic, PNAS, 2005). Recombinant virus was made using the Phoenix amphotropic packaging system. Culture supernatant containing retrovirus was used to infect C1498 cells in the presence of 5 μg/ml of hexadimethrine bromide (Sigma) or 12 μg/ml of retronectin (Takara). UL49.5-transduced cells expressing ΔNGFR were selected using a FACSVantage cell sorter (BD Biosciences).

Metabolic labeling

Cells were depleted of Met and Cys for 30 min, and labeled with EasyTag Express ^{35}S protein labeling mix (PerkinElmer) for 10 min at 200 μCi/ml. Radioactive medium was immediately removed by centrifugation, and the labeled cells were chased in the presence of excess Met and Cys (5 mM each) for the indicated periods of time. Cells were washed extensively and subjected to immunoprecipitation.

Immunoprecipitation

Cells were lysed in 1% NP-40 (Sigma) in tris-buffered saline (TBS) (10 mM Tris pH 7.6, 150 mM NaCl) with protease inhibitor cocktail (Roche). For the co-immunoprecipiation experiments, TBS containing 1% digitonin (Wako) and 20 mM iodoacetamide (Sigma) was used for cell lysis. Postnuclear lysate was incubated for 2 h at 4°C with Protein A agarose (RepliGen) that was pre-incubated with one of the following antibodies: rabbit anti-K^{b} serum, rabbit anti-mouse TAP1 serum (Lybarger et al., 2003), or anti-HA 16B12 (Covance). Where indicated, eluted proteins were treated with 10 mU of Endoglycosidase H (Roche) for 2 h at 37°C prior to SDS-PAGE.

Immunoblotting

Proteins separated by SDS-PAGE were transferred on the PVDF membranes (Millipore). Blots were incubated with one of the following primary antibodies, rabbit anti-K^{b} serum, rabbit anti-TAP1 serum, rabbit anti-calreticulin (Stressgen), or rabbit anti-HA (Covance), in combination

with horseradish peroxidase (HRP)-conjugated goat anti-rabbit IgG (Amersham Biosciences). To detect tapasin, blots were incubated with hamster anti-mouse tapasin 5D3 followed by biotinylated goat anti-hamster Ig and HRP-streptavidin. Band intensities on the films were quantified by ImageQuant TL software (Amersham Biosciences).

Measuring MHC class I thermostability

Cells were metabolically labeled for 10 min as described and chased for 30 min. After stringent washing, cells were lysed with ice-cold TBS containing 1% NP-40. Lysates were incubated with 0, 10^2, 10^4 nM of VNVDYSKL peptide at 4°C for 1 h, followed by incubation at 37°C for 30 min. Lysates were cooled on ice for 5 min and subjected to immunoprecipitation with anti-K^b antibody B8-24-3 (ATCC).

Peptide Transport Assay

Cells were permeabilized using Streptolysin-O (Murex Diagnostics) at 37°C for 10 min, followed by incubation with 4.5 μM of the fluorescein-conjugated synthetic peptide CVNKTERAY (*N*-core glycosylation site underlined) in the presence of 10 mM ATP or 0.125 M EDTA at 37°C for 10 min. Peptide translocation was terminated by adding ice-cold lysis buffer containing 1% Triton X-100. Glycosylated peptides were retrieved from post-nuclear lysates by incubation with concanavalin A sepharose beads (GE Healthcare) for 2 h at 4°C. After washing, peptides were eluted from the beads with elution buffer (500 mM mannopyranoside, 10 mM EDTA, 50 mM Tris HCl pH 8.0) for 1 h at room temperature. Fluorescence was measured using a Mithras LB 940 multilabel reader (Berthold Technologies).

Mice, infection, and depletion of CD8 T cells

Female C57BL/6 mice were purchased from National Cancer Institute. Mice were maintained under specific pathogen–free conditions and used when they were 9 weeks old. Mice under anesthesia were inoculated intranasally with 20 μl of virus diluted in PBS. Survival was monitored for 4 weeks following infection. For CD8-depletion studies, 1 mg of H35, a monoclonal antibody specific for CD8β (Smith and Allen, 1991), or SFR3-DR5 (ATCC HB-151), an IgG2b isotype-control, was administered to each mouse intraperitoneally every fourth day starting two days prior to CPXV infection. Depletion efficiency was > 95%, as determined by flow cytometry. Animal studies were approved by the Animal Studies Committee at Washington University in St. Louis.

IFN-γ production assay and cytotoxicity assay

C57BL/6 mice were intranasally infected with 1×10^4 PFU of CPXV, and splenocytes were harvested at day 7 post infection. MC57G cells were mock infected or infected with wtCPXV, CPXVΔ12, CPXVΔ203, or CPXVΔ12Δ203 at a multiplicity of infection (MOI) of 2, and harvested at 16 h post-infection. To measure IFN-γ production by CD8 T cells, we incubated splenocytes (1×10^6) with MC57G cells (3×10^5) for 1 h, and then further incubated in the presence of GolgiPlug (BD Biosciences) for an additional 6 h. Cells were stained for CD3, CD8, and intracellular IFN-γ, and analyzed by flow cytometry. For cytotoxicity assays, ^{51}Cr-labeled MC57G cells (1×10^5) were incubated with splenocytes at different effector to target ratios for 4 h. ^{51}Cr-release was measured using γ-counter. Percent lysis was calculated by 100× (experimental release – spontaneous release)/(maximum release – spontaneous release). Spontaneous release represents background radioactive counts from the targets alone, and maximum release represents the counts from NP-40-lysed target cells.

One-step growth curve

Vero cells were infected with wtCPXV, CPXVΔ12Δ203, or CPXV^{R}12^{R}203 at a MOI of 5. Cells were harvested at 1, 8, 12, 24 h post infection and CPXV genome copy numbers were quantified by quantitative PCR as explained below.

Quantification of CPXV genome copy number

CPXV genome copy was quantified by quantitative PCR with a forward primer (5′-CGGCTAAGAGTTGCACATCCA-3′) and a reverse primer (5′-TCTGCTCCATTTAGTACCGATTCTAG-3′) hybridized at positions 2048–2068 and 2092–2118, respectively, and a probe (5′-AGGACGTAGAATGATCTTGTA-3′) at position 2070–2091. Serial 10-fold dilutions of the positive-control plasmid, which was generated by cloning the amplicon (2048–2118) into pBluscriptII, were used to derive a standard curve for quantification. For splenic virus titers, spleens were harvested at day 7 or 10 post infection, weighed individually, homogenized in Eagle's minimum medium (Cellgro) containing 2% fetal calf serum, and kept frozen until use. Upon thawing, genomic DNA was purified using DNeasy Blood & Tissue kit, and genome copy numbers were determined by quantitative PCR.

Supplementary Material

Refer to Web version on PubMed Central for supplementary material.

Acknowledgments

This work was supported by the Midwest Regional Center of Excellence for Biodefense (NIH U54-AI057160), and the Barnes-Jewish Hospital Foundation. W.M.Y. is an investigator of the Howard Hughes Medical Institute. T.H.H. is supported by NIH grant AI019687.

References

Ahn K, Angulo A, Ghazal P, Peterson PA, Yang Y, Fruh K. Human cytomegalovirus inhibits antigen presentation by a sequential multistep process. Proc Natl Acad Sci U S A 1996a;93:10990–10995. [PubMed: 8855296]

Ahn K, Gruhler A, Galocha B, Jones TR, Wiertz EJ, Ploegh HL, Peterson PA, Yang Y, Fruh K. The ER-luminal domain of the HCMV glycoprotein US6 inhibits peptide translocation by TAP. Immunity 1997;6:613–621. [PubMed: 9175839]

Ahn K, Meyer TH, Uebel S, Sempe P, Djaballah H, Yang Y, Peterson PA, Fruh K, Tampe R. Molecular mechanism and species specificity of TAP inhibition by herpes simplex virus ICP47. EMBO J 1996b; 15:3247–3255. [PubMed: 8670825]

Andersson M, Paabo S, Nilsson T, Peterson PA. Impaired intracellular transport of class I MHC antigens as a possible means for adenoviruses to evade immune surveillance. Cell 1985;43:215–222. [PubMed: 2934137]

Boname JM, de Lima BD, Lehner PJ, Stevenson PG. Viral degradation of the MHC class I peptide loading complex. Immunity 2004;20:305–317. [PubMed: 15030774]

Bouvier M, Wiley DC. Importance of peptide amino and carboxyl termini to the stability of MHC class I molecules. Science 1994;265:398–402. [PubMed: 8023162]

Byun M, Wang X, Pak M, Hansen TH, Yokoyama WM. Cowpox virus exploits the endoplasmic reticulum retention pathway to inhibit MHC class I transport to the cell surface. Cell Host Microbe 2007;2:306–315. [PubMed: 18005752]

Campbell JA, Trossman DS, Yokoyama WM, Carayannopoulos LN. Zoonotic orthopoxviruses encode a high-affinity antagonist of NKG2D. J Exp Med 2007;204:1311–1317. [PubMed: 17548517]

Chantrey J, Meyer H, Baxby D, Begon M, Bown KJ, Hazel SM, Jones T, Montgomery WI, Bennett M. Cowpox: reservoir hosts and geographic range. Epidemiol Infect 1999;122:455–460. [PubMed: 10459650]

Coscoy L, Ganem D. Kaposi's sarcoma-associated herpesvirus encodes two proteins that block cell surface display of MHC class I chains by enhancing their endocytosis. Proc Natl Acad Sci U S A 2000;97:8051–8056. [PubMed: 10859362]

Dasgupta A, Hammarlund E, Slifka MK, Fruh K. Cowpox virus evades CTL recognition and inhibits the intracellular transport of MHC class I molecules. J Immunol 2007;178:1654–1661. [PubMed: 17237415]

Doom CM, Hill AB. MHC class I immune evasion in MCMV infection. Med Microbiol Immunol 2008;197:191–204. [PubMed: 18330598]

Fahnestock ML, Tamir I, Narhi L, Bjorkman PJ. Thermal stability comparison of purified empty and peptide-filled forms of a class I MHC molecule. Science 1992;258:1658–1662. [PubMed: 1360705]

Fruh K, Ahn K, Djaballah H, Sempe P, van Endert PM, Tampe R, Peterson PA, Yang Y. A viral inhibitor of peptide transporters for antigen presentation. Nature 1995;375:415–418. [PubMed: 7760936]

Goldsmith K, Chen W, Johnson DC, Hendricks RL. Infected cell protein (ICP)47 enhances herpes simplex virus neurovirulence by blocking the CD8+ T cell response. J Exp Med 1998;187:341–348. [PubMed: 9449714]

Guerin JL, Gelfi J, Boullier S, Delverdier M, Bellanger FA, Bertagnoli S, Drexler I, Sutter G, Messud-Petit F. Myxoma virus leukemia-associated protein is responsible for major histocompatibility complex class I and Fas-CD95 down-regulation and defines scrapins, a new group of surface cellular receptor abductor proteins. J Virol 2002;76:2912–2923. [PubMed: 11861858]

Guidotti LG, Chisari FV. To kill or to cure: options in host defense against viral infection. Curr Opin Immunol 1996;8:478–483. [PubMed: 8794011]

Hansen TH, Bouvier M. MHC class I antigen presentation: learning from viral evasion strategies. Nat Rev Immunol. 2009

Hengel H, Koopmann JO, Flohr T, Muranyi W, Goulmy E, Hammerling GJ, Koszinowski UH, Momburg F. A viral ER-resident glycoprotein inactivates the MHC-encoded peptide transporter. Immunity 1997;6:623–632. [PubMed: 9175840]

Hill A, Jugovic P, York I, Russ G, Bennink J, Yewdell J, Ploegh H, Johnson D. Herpes simplex virus turns off the TAP to evade host immunity. Nature 1995;375:411–415. [PubMed: 7760935]

Hislop AD, Ressing ME, van Leeuwen D, Pudney VA, Horst D, Koppers-Lalic D, Croft NP, Neefjes JJ, Rickinson AB, Wiertz EJ. A CD8+ T cell immune evasion protein specific to Epstein-Barr virus and its close relatives in Old World primates. J Exp Med 2007;204:1863–1873. [PubMed: 17620360]

Ishido S, Wang C, Lee BS, Cohen GB, Jung JU. Downregulation of major histocompatibility complex class I molecules by Kaposi's sarcoma-associated herpesvirus K3 and K5 proteins. J Virol 2000;74:5300–5309. [PubMed: 10799607]

Jones TR, Wiertz EJ, Sun L, Fish KN, Nelson JA, Ploegh HL. Human cytomegalovirus US3 impairs transport and maturation of major histocompatibility complex class I heavy chains. Proc Natl Acad Sci U S A 1996;93:11327–11333. [PubMed: 8876135]

Karupiah G, Buller RM, Van Rooijen N, Duarte CJ, Chen J. Different roles for CD4+ and CD8+ T lymphocytes and macrophage subsets in the control of a generalized virus infection. J Virol 1996;70:8301–8309. [PubMed: 8970949]

Koppers-Lalic D, Reits EA, Ressing ME, Lipinska AD, Abele R, Koch J, Marcondes Rezende M, Admiraal P, van Leeuwen D, Bienkowska-Szewczyk K, et al. Varicelloviruses avoid T cell recognition by UL49.5-mediated inactivation of the transporter associated with antigen processing. Proc Natl Acad Sci U S A 2005;102:5144–5149. [PubMed: 15793001]

Koppers-Lalic D, Verweij MC, Lipinska AD, Wang Y, Quinten E, Reits EA, Koch J, Loch S, Rezende MM, Daus F, et al. Varicellovirus UL 49.5 proteins differentially affect the function of the transporter associated with antigen processing, TAP. PLoS Pathog 2008;4:e1000080. [PubMed: 18516302]

Lehner PJ, Karttunen JT, Wilkinson GW, Cresswell P. The human cytomegalovirus US6 glycoprotein inhibits transporter associated with antigen processing-dependent peptide translocation. Proc Natl Acad Sci U S A 1997;94:6904–6909. [PubMed: 9192664]

Liu H, Fu J, Bouvier M. Allele- and locus-specific recognition of class I MHC molecules by the immunomodulatory E3-19K protein from adenovirus. J Immunol 2007;178:4567–4575. [PubMed: 17372015]

Liu X, Kremer M, Broyles SS. A natural vaccinia virus promoter with exceptional capacity to direct protein synthesis. J Virol Methods 2004;122:141–145. [PubMed: 15542137]

Lybarger L, Wang X, Harris MR, Virgin HWt, Hansen TH. Virus subversion of the MHC class I peptide-loading complex. Immunity 2003;18:121–130. [PubMed: 12530981]

Machold RP, Wiertz EJ, Jones TR, Ploegh HL. The HCMV gene products US11 and US2 differ in their ability to attack allelic forms of murine major histocompatibility complex (MHC) class I heavy chains. J Exp Med 1997;185:363–366. [PubMed: 9016885]

Peaper DR, Cresswell P. Regulation of MHC class I assembly and peptide binding. Annu Rev Cell Dev Biol 2008;24:343–368. [PubMed: 18729726]

Reusch U, Muranyi W, Lucin P, Burgert HG, Hengel H, Koszinowski UH. A cytomegalovirus glycoprotein re-routes MHC class I complexes to lysosomes for degradation. EMBO J 1999;18:1081–1091. [PubMed: 10022849]

Schumacher TN, Heemels MT, Neefjes JJ, Kast WM, Melief CJ, Ploegh HL. Direct binding of peptide to empty MHC class I molecules on intact cells and in vitro. Cell 1990;62:563–567. [PubMed: 2199065]

Seet BT, Johnston JB, Brunetti CR, Barrett JW, Everett H, Cameron C, Sypula J, Nazarian SH, Lucas A, McFadden G. Poxviruses and immune evasion. Annu Rev Immunol 2003;21:377–423. [PubMed: 12543935]

Smith SC, Allen PM. Myosin-induced acute myocarditis is a T cell-mediated disease. J Immunol 1991;147:2141–2147. [PubMed: 1918949]

Stevenson PG, Efstathiou S, Doherty PC, Lehner PJ. Inhibition of MHC class I-restricted antigen presentation by gamma 2-herpesviruses. Proc Natl Acad Sci U S A 2000;97:8455–8460. [PubMed: 10890918]

Stevenson PG, May JS, Smith XG, Marques S, Adler H, Koszinowski UH, Simas JP, Efstathiou S. K3-mediated evasion of CD8(+) T cells aids amplification of a latent gamma-herpesvirus. Nat Immunol 2002;3:733–740. [PubMed: 12101398]

Wagner M, Gutermann A, Podlech J, Reddehase MJ, Koszinowski UH. Major histocompatibility complex class I allele-specific cooperative and competitive interactions between immune evasion proteins of cytomegalovirus. J Exp Med 2002;196:805–816. [PubMed: 12235213]

Wiertz EJ, Jones TR, Sun L, Bogyo M, Geuze HJ, Ploegh HL. The human cytomegalovirus US11 gene product dislocates MHC class I heavy chains from the endoplasmic reticulum to the cytosol. Cell 1996a;84:769–779. [PubMed: 8625414]

Wiertz EJ, Tortorella D, Bogyo M, Yu J, Mothes W, Jones TR, Rapoport TA, Ploegh HL. Sec61-mediated transfer of a membrane protein from the endoplasmic reticulum to the proteasome for destruction. Nature 1996b;384:432–438. [PubMed: 8945469]

Williams AP, Peh CA, Purcell AW, McCluskey J, Elliott T. Optimization of the MHC class I peptide cargo is dependent on tapasin. Immunity 2002;16:509–520. [PubMed: 11970875]

York IA, Roop C, Andrews DW, Riddell SR, Graham FL, Johnson DC. A cytosolic herpes simplex virus protein inhibits antigen presentation to CD8+ T lymphocytes. Cell 1994;77:525–535. [PubMed: 8187174]

Ziegler H, Thale R, Lucin P, Muranyi W, Flohr T, Hengel H, Farrell H, Rawlinson W, Koszinowski UH. A mouse cytomegalovirus glycoprotein retains MHC class I complexes in the ERGIC/cis-Golgi compartments. Immunity 1997;6:57–66. [PubMed: 9052837]

Zuniga MC, Wang H, Barry M, McFadden G. Endosomal/lysosomal retention and degradation of major histocompatibility complex class I molecules is induced by myxoma virus. Virology 1999;261:180–192. [PubMed: 10497104]

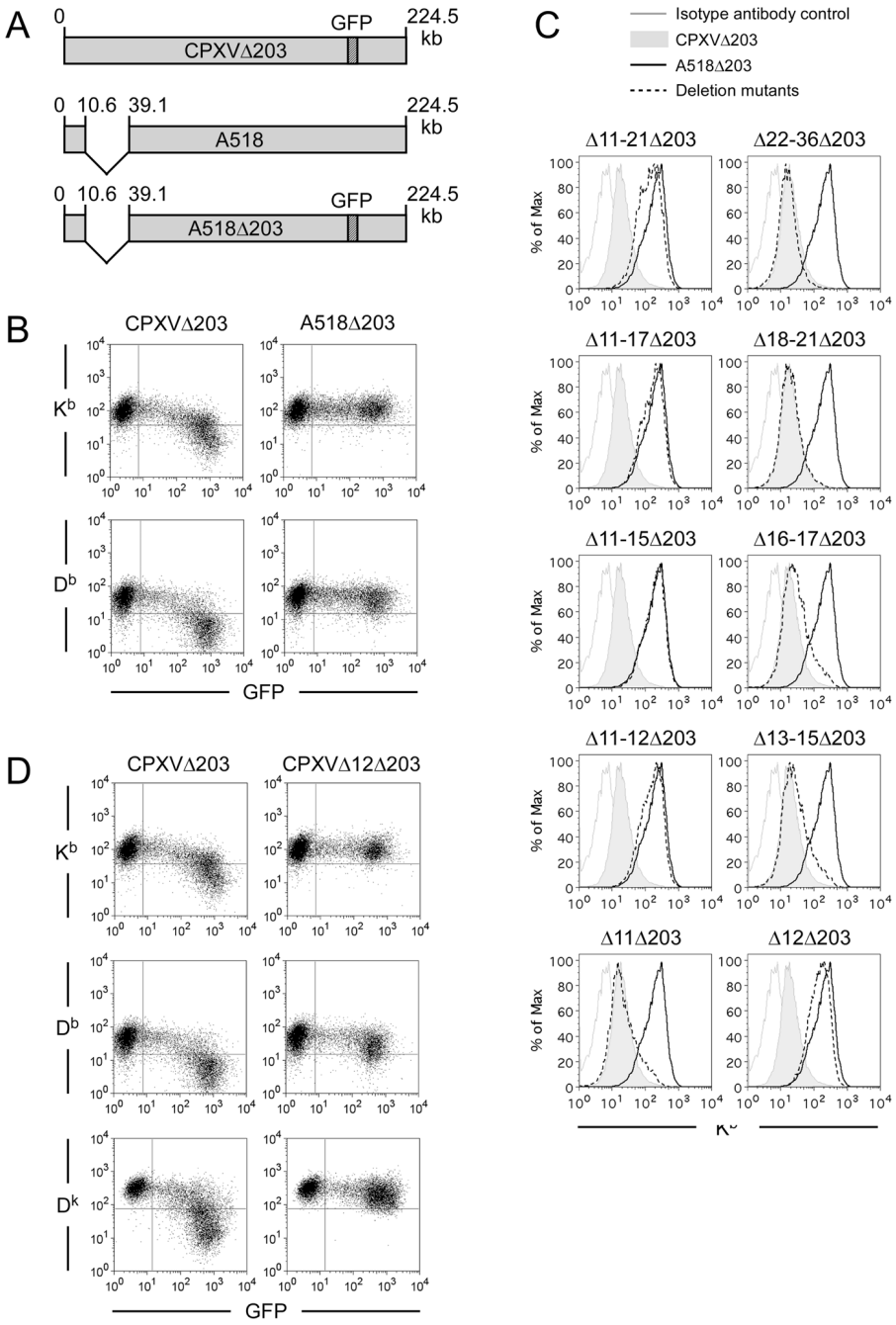

Figure 1. Identification of CPXV12 by loss-of-function screening

(A) Schematic diagram of CPXV mutants. Numbers indicate positions in kilobase (kb) corresponding to the wild-type CPXV strain Brighton Red genome. CPXV203 was replaced with GFP in CPXVΔ203 and A518Δ203. (B) MC57G cells infected with indicated CPXV mutants were analyzed for surface K^b or D^b expression at 24 h post infection. (C) MC57G cells infected with CPXV mutants indicated above each histogram were harvested at 24 h post infection and their surface K^b expression levels were compared to those of CPXVΔ203- or A518Δ203-infected cells. (D) MC57G cells (K^b, D^b) and L929 cells (D^k) were infected with CPXVΔ203 or CPXVΔ12Δ203 and analyzed for MHC class I expression at 24 h post infection.

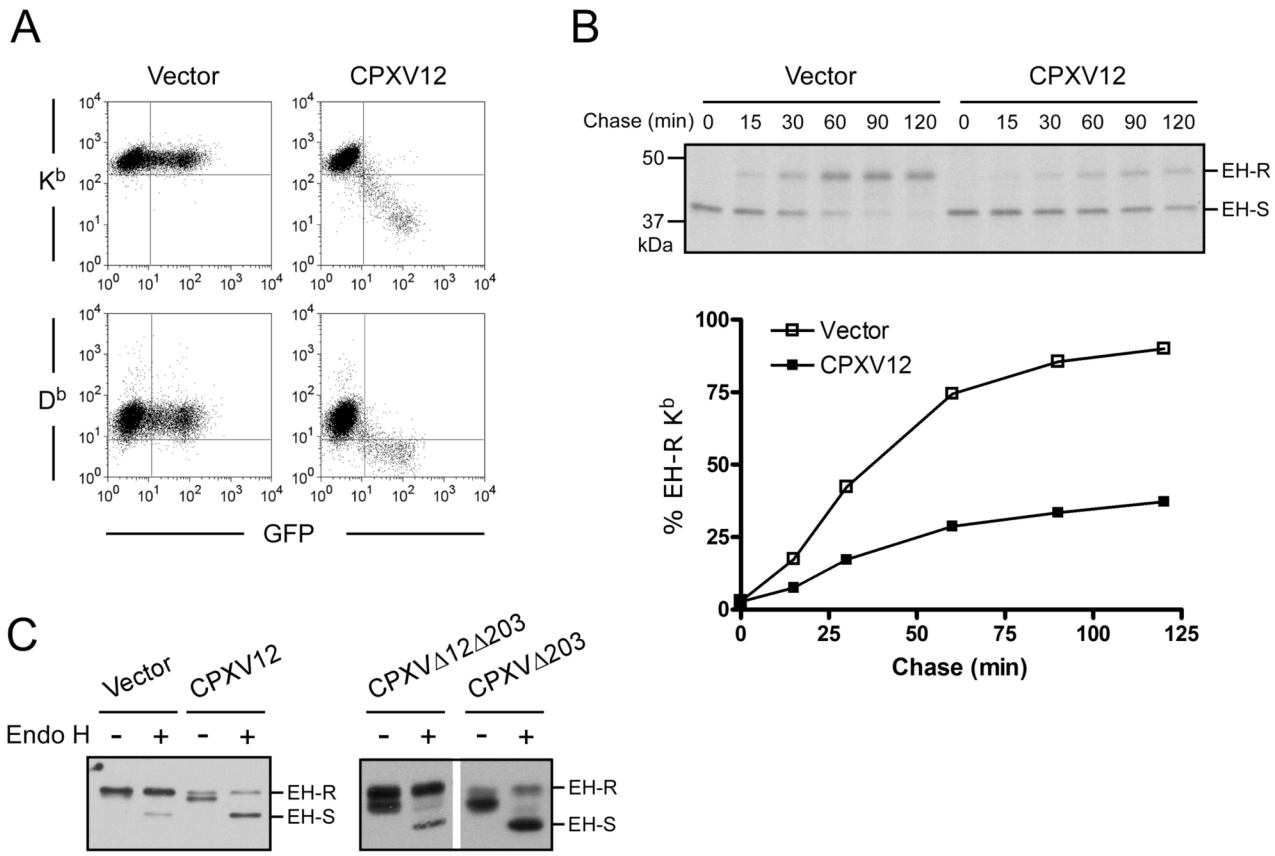

Figure 2. CPXV12 delays MHC class I trafficking

(A) Surface expression levels of K^b and D^b were measured in C1498 cells transduced with either vector alone or CPXV12. GFP serves as a marker for transduction.

(B) Intracellular trafficking of K^b molecules was examined in the presence and absence of CPXV12. C1498 cells transduced with either vector alone or CPXV12 were sorted several times until the GFP positive population was >95% (data not shown). They were labeled with [^{35}S]-Met/Cys for 10 min and chased for the indicated periods of time. K^b molecules were immunoprecipitated from cell lysates and treated with Endo H prior to SDS-PAGE. The proportion of Endo H-resistant form at each chase time point was plotted. A representative result of three independent experiments is shown. EH-R, Endo H-resistant; EH-S, Endo H-sensitive.

(C) C1498 cells transduced with either vector alone or CPXV12 were sorted several times until the GFP positive population was >95% (data not shown). MC57G cells were infected with either CPXVΔ12Δ203 or CPXVΔ203 at a MOI of 3. Cell lysates were treated with Endo H where indicated, and K^b heavy chain was detected by immunoblotting.

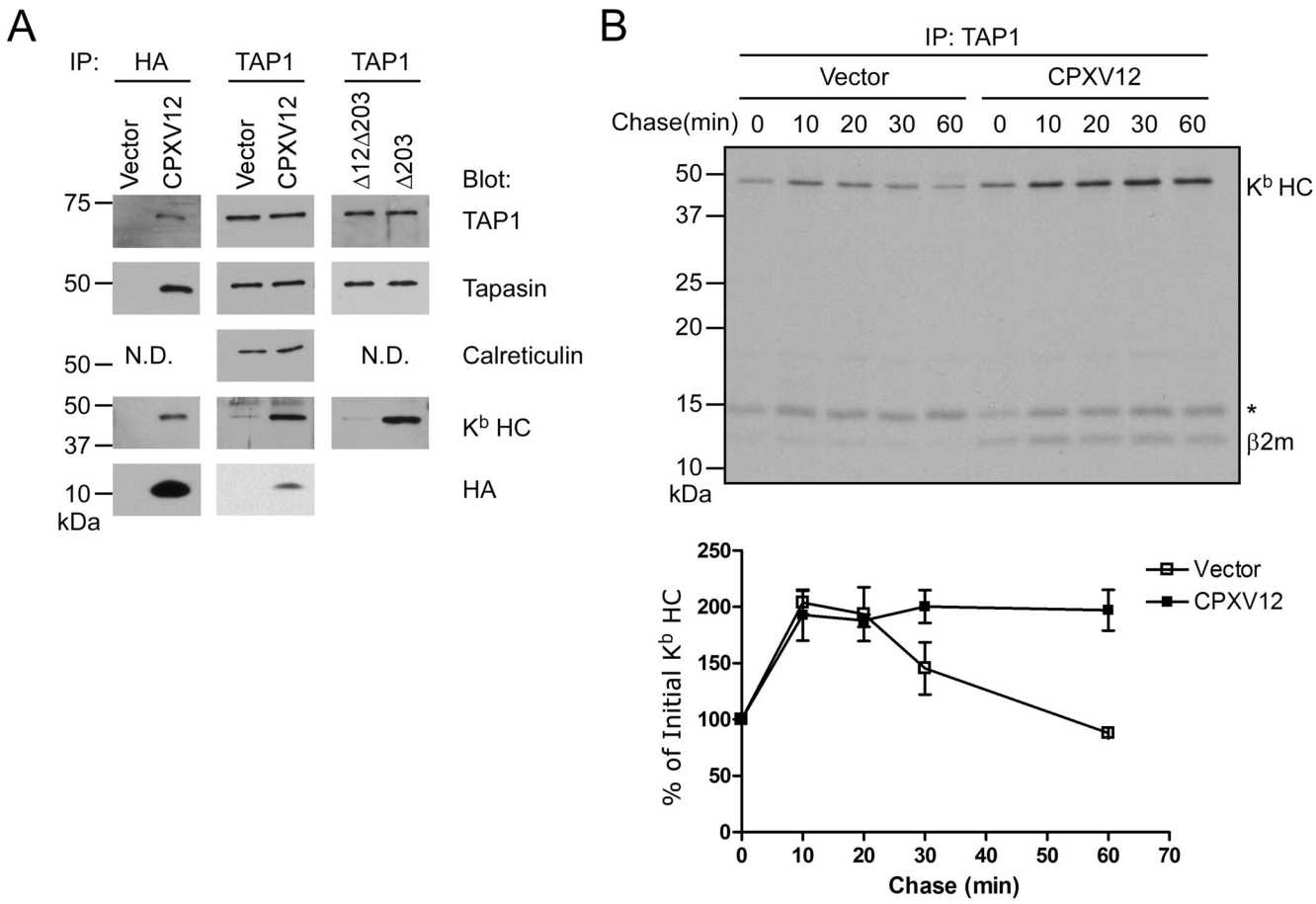

Figure 3. CPXV12 inhibits MHC class I dissociation from the PLC

(A) Digitonin lysates of C1498 cells transduced with either vector alone or CPXV12 (left four lanes) and of MC57G cells infected with either CPXVΔ12Δ203 or CPXVΔ203 (right two lanes) were subjected to immunoprecipitation with anti-HA or anti-TAP1 serum. Precipitated proteins were separated by SDS-PAGE and blotted for indicated proteins. N.D., not determined.

(B) C1498 cells transduced with either vector alone or CPXV12 were labeled with [^{35}S]-Met/Cys for 10 min, and then chased for the indicated periods of time. Cells were lysed with 1% digitonin, and subjected to immunoprecipitation with anti-TAP1 serum. From the co-precipitated proteins, K^b was further purified by re-immunoprecipitation with anti-K^b serum. Protein bands corresponding to K^b heavy chain (HC) and β2m are indicated. Asterisk (*) indicates non-specific protein. The levels of K^b heavy chain at each time-point compared to the initial amounts (set as 100%) are plotted in the bottom graph. Mean ± standard error of mean (SEM) from two independent experiments is shown.

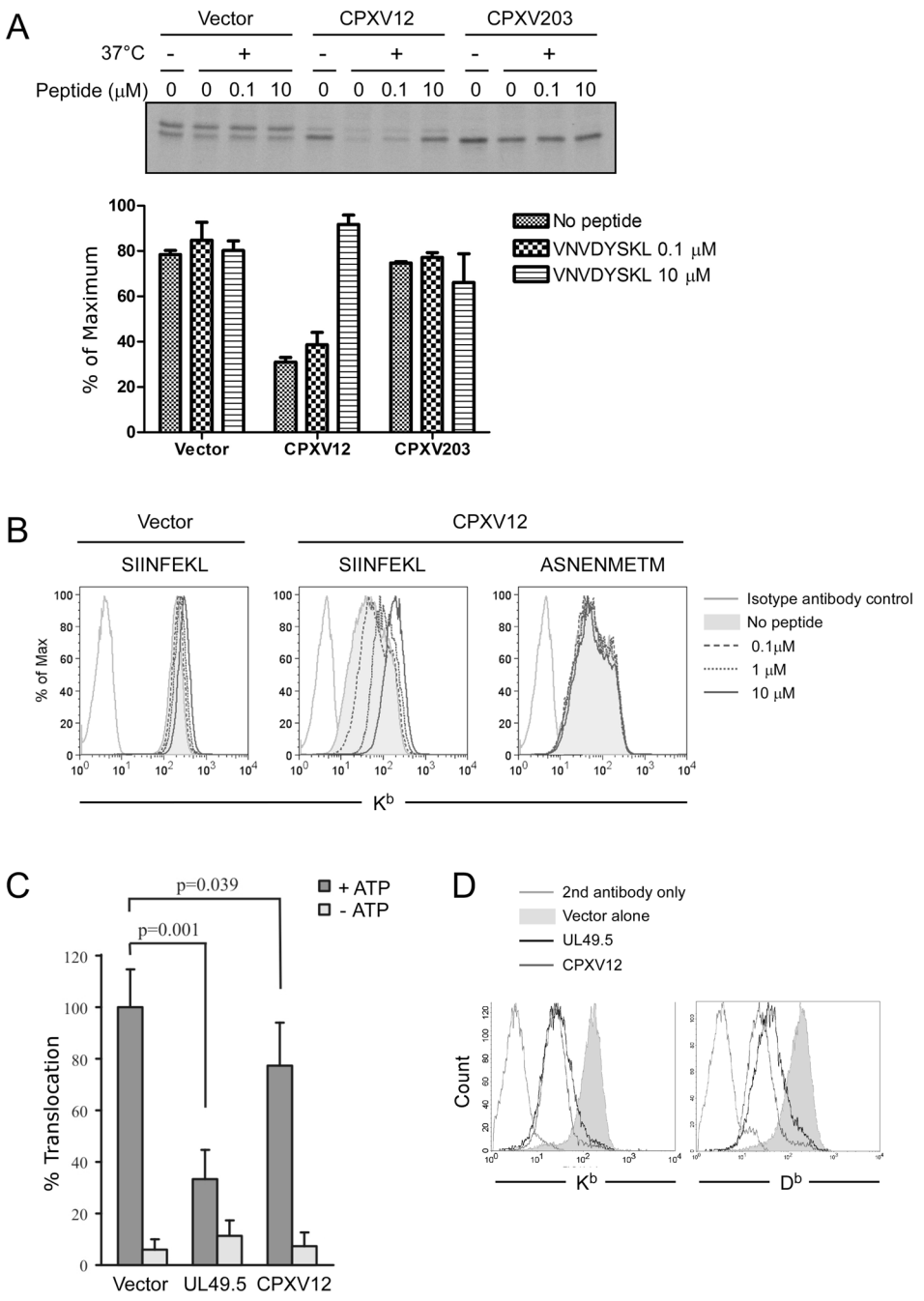

Figure 4. CPXV12 impairs peptide loading

(A) C1498 cells transduced with indicated constructs were labeled with [^{35}S]-Met/Cys for 10 min and chased for 60 min. Cell lysates were incubated with indicated concentrations of peptide VNVDYSKL at 4°C for 30 min, and subsequently incubated at 37°C for 30 min. K^b was immunoprecipitated with monoclonal antibody B8-24-3, which recognizes peptide-bound K^b. Band intensities were quantified and plotted as percent of maximum, which represents the amount of K^b before the 37°C-incubation (set as 100%). Mean ± SEM from three independent experiments is shown.

(B) C1498 cells transduced with vector alone or CPXV12 were incubated with indicated concentrations of SIINFEKL or ASNENMETM peptide in the culture medium for 16 h at 37° C, and analyzed for surface K^b expression by flow cytometry.
(C) Peptide transport activity of TAP was assessed in C1498 cells transduced with vector alone, BHV-1 UL49.5, or CPXV12. Translocation of the fluorescently-labeled peptide CVNKTERAY was evaluated in the presence or absence of ATP. Peptide transport is expressed as percentage of translocation, relative to the translocation observed in control cells (set as 100%). Statistical significance was determined by Student's t-test.
(D) Surface levels of K^b and D^b were compared between C1498 cells transduced with indicated constructs.

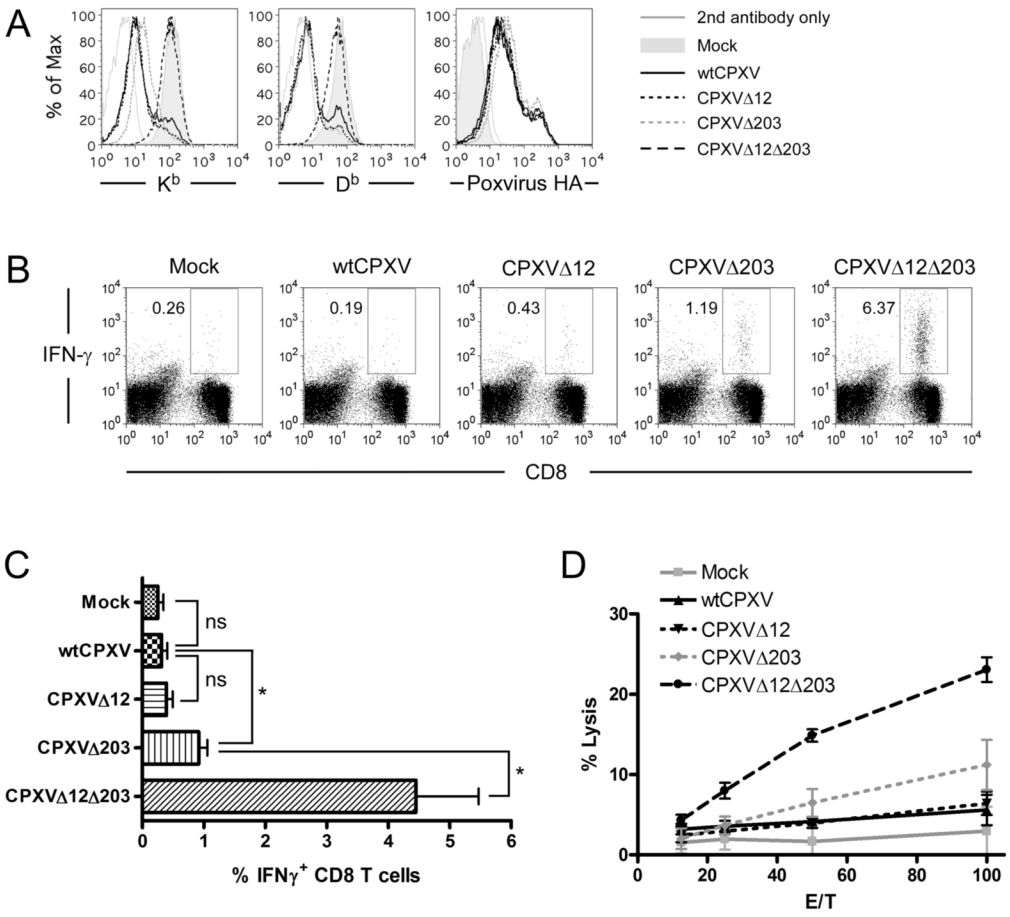

Figure 5. Evasion of antiviral CD8 T cell responses by CPXV12 and CPXV203

C57BL/6 mice were intranasally infected with 1×10^4 PFU of wtCPXV. Splenocytes were harvested at day 7 post infection. MC57G cells were mock infected or infected with indicated viruses at a MOI of 2 for 18 h.

(A) Surface expression levels of K^b, D^b, and poxvirus HA on MC57G cells were analyzed by flow cytometry.

(B) Splenocytes were incubated with MC57G cells for 7 h, and analyzed for IFN-γ by intracellular staining followed by flow cytometry. Numbers indicate percentage of IFN-γ^+ cells among total $CD8^+$ lymphocytes. A representative result of three similar experiments is shown.

(C) Same as (B) except mean ± SEM from three independent experiments is shown. Statistical significance was determined by Student's t-test. *, $p < 0.05$; ns, not significant.

(D) Splenocytes were co-incubated with ^{51}Cr-labeled MC57G cells for 4 h. Lysis of MC57G cells was measured by ^{51}Cr-release assay. E/T represents effector (splenocytes) to target (MC57G cells) ratio. Mean ± SEM from three independent experiments is shown.

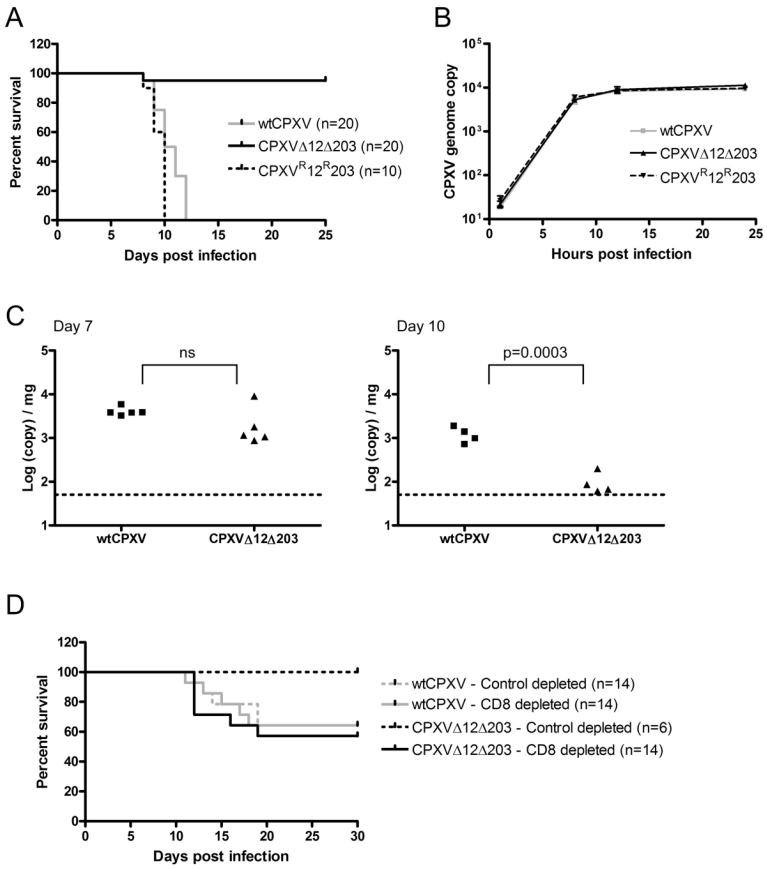

Figure 6. CPXV12 and CPXV203 abrogate CD8 T cell immunity against CPXV *in vivo*

(A) 9-week-old C57BL/6 mice were infected intranasally with 5×10^4 PFU of the indicated viruses and monitored for survival. Results were pooled from two independent experiments.
(B) One-step growth curves for the indicated viruses were obtained in Vero cells. Genome copy numbers were determined by quantitative PCR. Mean ± SEM of triplicates is shown.
(C) 9-week-old C57BL/6 mice were infected intranasally with indicated viruses. Spleens from infected mice were harvested at day 7 or day 10 post infection, and the viral loads were determined by quantitative PCR. Dotted lines indicate limits of detection. Statistical significance was determined by Student's t-test.
(D) 9-week-old C57BL/6 mice were infected intranasally with 1×10^4 PFU of the indicated viruses and monitored for survival. Starting two days prior to infection, mice were treated with 1 mg of either isotype-control or CD8-depleting antibody every fourth day throughout the monitoring period. Results were pooled from two independent experiments.